

Effect of multi-valve closure on superposed pressure in a tree-type long distance gravitational water supply system

Xingtao Wang, Jian Zhang, Xiaodong Yu, Sheng Chen, Wenlong Zhao and Hui Xu

ABSTRACT

Valves are installed at the end of each branch pipeline in a tree-type long distance gravitational water supply system to regulate flow. However, the sequential closing of all valves may cause a tremendous superposed pressure rise, even larger than the pressure rise under simultaneous valve closure. In this paper, the effects of sequential valve closure on the superposed maximum water hammer pressure rise in a pipeline were investigated. By using the wave superposition principle, a sequential valve closure formula leading to maximum water hammer was proposed and verified using numerical simulation based on a practical project. In addition, the superposed maximum pressure rises in the pipeline were compared under single, simultaneous and sequential valve closure, respectively. The results show that the sequential valve closure formula agrees well with the numerical results and the pressure rise in the pipeline under the sequential closing was the largest. Moreover, compared with the superposed maximum pressure rises at the main pipeline, the effect of sequential valve closure on superposed maximum pressure rise at the branch pipeline is more sensitive.

Key words | propagation and superposition of waves, single/simultaneous/sequential valve closure, tree-type gravitational water supply system, water hammer pressure

Xingtao Wang
Jian Zhang
Xiaodong Yu (corresponding author)
Sheng Chen
Wenlong Zhao
Hui Xu
College of Water Conservancy and Hydropower
Engineering,
Hohai University,
Nanjing City, Jiangsu Province 210098,
China
E-mail: yuxiaodong_851@hhu.edu.cn

INTRODUCTION

The severe shortage of water resources is a crucial issue all over the world for the accelerated construction of urbanization and the concentration of the population (Fan *et al.* 2019; Xiao *et al.* 2019). Through the construction of long distance water supply systems, transporting water resources from an area rich in water resources to the area with shortage of water is the most effective approach (Wang *et al.* 2018). The systems are mainly divided into pumping station pressurization and gravity flow. Compared with pumping station pressurization, because it relies on the topographical drop to supply water, the gravity flow has favorable economics. However, safety along the pipeline is a very serious challenge. In long distance gravitational water supply systems, each branch pipeline forms a branching junction

with the main pipeline, and valves are installed at the end of each branch pipeline to regulate flow (Zhang *et al.* 2018). When a valve is illegally closed, a positive water hammer wave is generated at the valve and propagates to the pipeline, and the wave may cause tremendous fluctuations of pressure along the pipeline. Then, when the maximum pressure exceeds the pressure standard of pipeline, a pipe burst will be caused, resulting in enormous damage to the pipeline system. Therefore, it is necessary to investigate how to effectively prevent illegal closure of the valves of a long distance gravitational water supply system.

In a long distance gravitational water supply system, it is generally accepted that valves are components that can effectively regulate flow (Miao *et al.* 2017; Lai *et al.* 2018).

In previous studies, the model design of the valves has been intensively investigated (Bostan *et al.* 2018). For instance, Liao *et al.* proposed a plane-sealed large flow directional valve with different throttle windows (Liao *et al.* 2017). Xu *et al.* introduced the structure and working principle of a contra-push check valve (Xu *et al.* 2011), and simulated the steady and transient characteristics of the check valve. In addition, there is a large number of published papers about the closing law of the valves in water supply systems (Zhang 2019). For example, Wang *et al.* (2017) proposed an improved two-segment closing law for a gravitational water supply system; the results showed that the closing law can effectively reduce the water hammer pressure caused by valve closing. Wan & Li (2016) studied the transient pressure, pump speed, and flow for various time differences and the valve opening process for the series pump–valve startup process. However, the above studies have focused on discussing the influence of closing law of a single valve on the water hammer pressure of water supply system, ignoring the impact of closing all valves between multiple branch pipelines.

Traditionally, the water hammer wave caused by valve closing propagates in a single pipeline without considering the effect of wave superposition and interference. Nevertheless, a long distance gravitational water supply system has many branch pipelines and water intakes. According to the propagation and superposition of the wave, the water hammer waves generated by closing valves are mutually strengthened or weakened by propagation and superposition along the pipelines. Typically, simultaneous closing of all valves is considered as the largest water hammer pressure rise case. However, as all branches have different distances from the water intakes, the time when the water hammer waves caused by the simultaneous closing of the valves arrive at a fixed section is different. Then, the water hammer waves cannot be strengthened when they are superposed to the same section. Hence, at a certain section, the superposed maximum pressure rise generated by the simultaneous closing of the valves may not be the largest. Therefore, motivated by the above discussion, this paper focuses on the closing law of valves and its influence on water hammer pressure in the tree-type long distance gravitational water supply system.

MATHEMATICAL MODEL

Transient flow model

The continuity and momentum equations are used to describe unsteady pipe flow (Wylie *et al.* 1993; Chaudhry 2014; Moghaddas *et al.* 2017).

$$\frac{Q}{A} \frac{\partial H}{\partial x} + \frac{\partial H}{\partial t} + \frac{a^2}{gA} \frac{\partial Q}{\partial x} - \frac{Q}{A} \sin \beta = 0 \quad (1)$$

$$g \frac{\partial H}{\partial x} + \frac{Q}{A^2} \frac{\partial Q}{\partial x} + \frac{1}{A} \frac{\partial Q}{\partial t} + \frac{fQ|Q|}{2DA^2} = 0 \quad (2)$$

where H is piezometric head (m), Q is discharge (m^3/s), D is pipe internal diameter (m), A is cross-sectional area (m^2), g is gravitational acceleration (m/s^2), a is wave speed (m/s), t is computational time (s), x is axial distance (m), f is friction coefficient, β is pipe slope.

Equations (1) and (2) can be converted to ordinary differential equations along the characteristic lines. Then, the characteristic equations can be obtained by integrating the ordinary differential equations.

The negative characteristic equation C^-

$$H_{Pi} = C_M + B_M Q_{Pi} \quad (3)$$

The positive characteristic equation C^+

$$H_{Pi} = C_P - B_P Q_{Pi} \quad (4)$$

where H_{Pi} is unknown piezometric head of section i at time t . Q_{Pi} is unknown discharge of section i at time t . C_M , B_M , C_P , and B_P are known constants in compatibility equations. Their values in the C^+ and C^- compatibility equations are, respectively: $C_M = H_{i+1} - BQ_{i+1}$, $B_M = B + R|Q_{i+1}|$, $C_P = H_{i-1} - BQ_{i-1}$, and $B_P = B + R|Q_{i-1}|$, where $B = a/gA$, $R = f\Delta x/2gDA^2$ and $\Delta t = \Delta x/a$.

Valve model

Valves are important components for regulating flow in fluid delivery systems such as petroleum, chemical, power plants and long distance water supply systems. Generally, the

discharge rate of a valve is determined by the pressure difference between the inlet and outlet, the valve opening and diameter of the valve. The pressure and discharge at the inlet and outlet can be solved through the characteristic lines on both sides of the valve.

The discharge value is determined by the coefficient of discharge and pressure difference of the valve. The relationship between the head and discharge may be written as

$$Q_{PV} = C_d A_{rV} \sqrt{2g\Delta H_{PV}} \tag{5}$$

where C_d is the coefficient of discharge and is a variable related to valve opening. Q_{PV} is the discharge of the valve (m^3/s), A_{rV} is the area of the valve opening (m^2), ΔH_{PV} is the losses at the valve (m).

C_d can be converted by the following

$$C_d = \frac{1}{\sqrt{\varepsilon}} \tag{6}$$

$$\varepsilon = 2gA_{rV}^2 \Delta H_{PV} Q_{PV}^2 \tag{7}$$

where ε is the loss coefficient of the valve.

Through Equations (3) and (4):

$$Q_{PV} = \frac{C_P - C_M}{B_P + B_M + \frac{\varepsilon|Q_{PV}|}{2gA_{rV}^2}} \tag{8}$$

where the Δt is small, the Q_{PV} on the right side of Equation (8) can be replaced by the instantaneous discharge rate Q_{PV0} at the time $t_0 = t - \Delta t$. Therefore, the discharge on the left

side can be directly obtained, and the values of H_{P1} and H_{P2} are determined.

INFLUENCE OF MULTI-VALVE CLOSING LAW ON WATER HAMMER WAVE

According to the wave independent propagation principle, when the waves propagate to a point in a pipeline, the vibration at this point is the superposition of the vibration caused by the individual water hammer waves alone. As shown in Figure 1(a), the two water hammer waves S_1 and S_2 with the same frequency are generated by the closing valve. The vibration equations can be written as:

$$\begin{cases} y_{10}(S_1, t) = A_{10} \cos(at + \varphi_{10}) \\ y_{20}(S_2, t) = A_{20} \cos(at + \varphi_{20}) \end{cases} \tag{9}$$

where y_{10} and y_{20} denote the vibration equations of S_1 and S_2 ; A_{10} and A_{20} are amplitudes of vibration equations; and φ_{10} and φ_{20} are the phases of the vibration equation.

When the two water hammer waves propagate to point P , the vibration equations can be written as:

$$\begin{cases} y_1(P, t) = A_1 \cos\left(at + \varphi_{10} - \frac{2\pi}{\lambda}r_1\right) \\ y_2(P, t) = A_2 \cos\left(at + \varphi_{20} - \frac{2\pi}{\lambda}r_2\right) \end{cases} \tag{10}$$

where y_1 and y_2 are the vibration equations of S_1 and S_2 at point P , respectively; A_1 and A_2 are amplitudes of vibration equations, respectively; λ is wavelength; and r_1 and r_2 are the distances from S_1 and S_2 to point P , respectively.

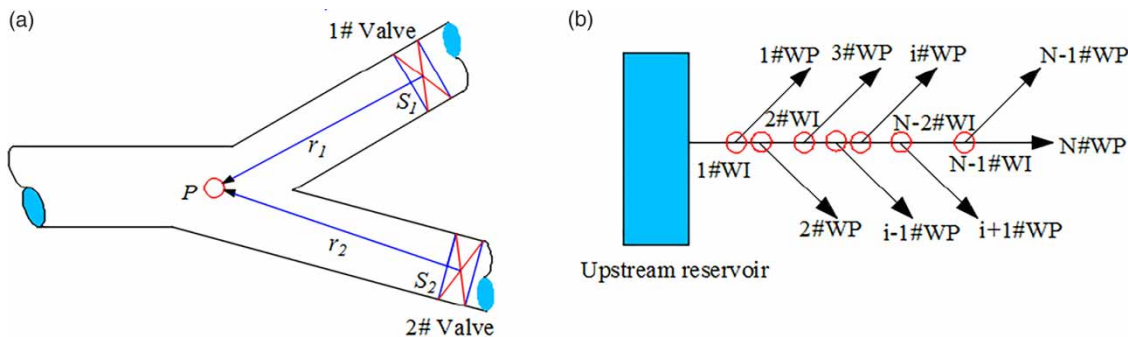


Figure 1 | (a) Superposition of water hammer wave, (b) gravitational water supply system layout (WP is water plant, WI is water intake).

According to Equation (10), the superposition vibration equation of the two waves at point P can be written as:

$$y = y_1 + y_2 = A \cos(at + \Delta\varphi) \quad (11)$$

where

$$\Delta\varphi = (\varphi_{20} - \varphi_{10}) - \frac{2\pi}{\lambda}(r_2 - r_1)$$

$$A^2 = A_1^2 + A_2^2 + 2A_1A_2 \cos\Delta\varphi$$

and $\Delta\varphi$ is the phase difference of the vibration equation.

The intensity of the wave is proportional to the square of the amplitude. Then, the intensity of the superimposed water hammer wave can be written as:

$$I = I_1 + I_2 + 2\sqrt{I_1 I_2} \cos\Delta\varphi \quad (12)$$

where I_1 and I_2 are the vibration intensities of S_1 and S_2 , respectively.

When the water hammer waves propagate in the same pipe, firstly, the frequency of propagation period is the same because the distance between two water hammer waves is equal. Secondly, in a fixed pipeline, the propagation direction of the water hammer wave is unidirectional. Therefore, the wave is either a positive or a negative, which spreads in the same direction. Thirdly, the phase difference of the waves at the same pipe in the same direction or reverse propagation is also constant. Therefore, the conditions of wave interference can be satisfied when the water hammer waves are propagating in a pipeline.

If $\Delta\varphi = \pm 2k\pi$, in which $k = 0, 1, 2, 3, \dots$, the superposition water hammer wave is strengthened. $A = A_{\max} = A_1 + A_2$, $I = I_{\max} = I_1 + I_2 + 2\sqrt{I_1 I_2}$, A_{\max} , I_{\max} are the maximum values of amplitude and vibration intensity of S_1 and S_2 at point P , respectively.

If $\Delta\varphi = \pm(2k+1)\pi$, in which $k = 0, 1, 2, 3, \dots$, the superposition water hammer wave is weakened. $A = A_{\min} = |A_1 - A_2|$, $I = I_{\min} = I_1 + I_2 - 2\sqrt{I_1 I_2}$, A_{\min} , I_{\min} are the minimum values of amplitude and vibration intensity of S_1 and S_2 at point P , respectively.

According to the prior works, the superposed pressure produced by simultaneous valves closure is the largest. However, the long distance gravitational water supply system has

many tree-type branches. All branches have different distances from the water intakes, and the time when the waves propagate to the same section is also different. Then the water hammer waves cannot be strengthened. Therefore, at the same section, the superposed pressure generated by the simultaneous valves closure is not the largest. According to the propagation, superposition and interference conditions of wave, when the waves can propagate to a fixed section at the same time, the amplitude of the superposition water hammer wave can reach the maximum value.

The tree-type long distance gravitational flow layout is shown in Figure 1(b). The system consists of N branch pipelines and $N - 1$ water intakes. Valves are installed at the end of each branch to regulate the flow.

It is assumed that the closing law of each valve is the same. The maximum water hammer pressure rise at the j th water intake generated by the closing valve of the i th valve is $H_{j,i}$, in which $1 \ll i \ll N$, $1 \ll j \ll N - 1$. And the time to reach the maximum water hammer pressure is $T_{j,i}$. According to the propagation of the wave, under the same type of pipeline, the farther the water intake is from the valve, the later the moment when the maximum pressure occurs. Therefore, the valve close to the water intake needs to be closed late. In other words, the farther the position of the valve is from the position of the maximum pressure, the earlier the valve needs to be closed.

If $T_{j,n} \gg T_{j,i}$, in which n is the n th valve, $T_{j,n}$ is the largest time to reach the maximum water hammer pressure at the j th water intake. Then, the closing law of the i th valve is:

$$\Delta T_{j,i} = T_{j,n} - T_{j,i} \quad (13)$$

where $\Delta T_{j,i}$ is the time when the i th valve is delayed compared with the n th valve.

Based on Equation (13), it can be obtained that the superposition maximum pressure rise at the j th water intake is:

$$\begin{cases} \Delta H_j \geq \sum_i^N H_{j,i} \\ \Delta H_j \geq \Delta H_{j,\text{all}} \end{cases} \quad (14)$$

where ΔH_j is the superposed maximum pressure rise at the j th water intake under the sequential valves closure. $\sum_i^N H_{j,i}$ is the superposed maximum pressure rise at the j th water intake

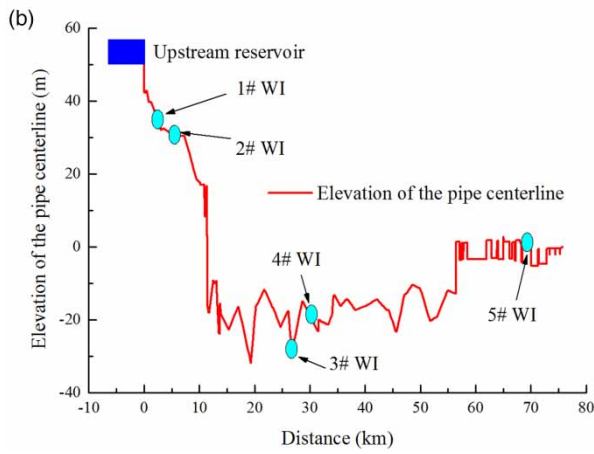
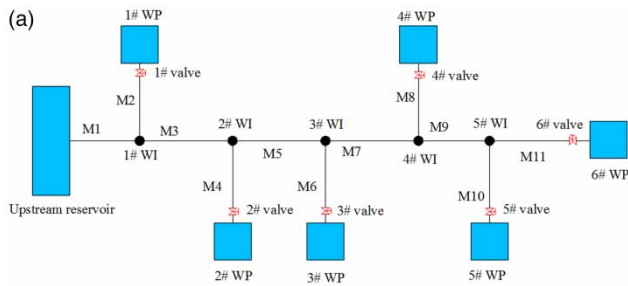


Figure 2 | (a) Layout of the water supply system, (b) elevation of main pipeline centerline and position of water intakes.

under the single valves closure. $\Delta H_{j,\text{all}}$ is the superposed maximum pressure rise at the j th water intake under the simultaneous valves closure.

CASE STUDY AND ANALYSIS

Figure 2(a) shows the layout of a tree-type long distance gravitational water supply system. The parameters of the system are shown in Table 1. The system takes water from the upstream reservoir, conveying water to downstream water plants by gravity in a pipe, with the total design

Table 1 | Parameters of the pipeline system

Pipe number	M1	M2	M3	M4	M5	M6	M7	M8	M9	M10	M11
Length (km)	2.142	2.393	1.207	8.850	25.634	4.910	3.068	6.410	39.610	1.193	4.451
Diameter (m)	6.0	2.8	6.0	3.5	3.4	2.4	3.4	0.6	3.2	1.2	3.2
Discharge (m^3/s)	43.3	7.6	35.7	18.3	17.4	3.2	14.2	5.1	9.1	0.8	8.3

Table 2 | Parameters of the maximum water hammer pressure rise and time at the 5# water intake

Valve	1#	2#	3#	4#	5#	6#
The maximum pressure (m)	42.64	47.50	50.99	59.19	44.17	142.48
$H_{5,i}$ (m)	2.38	7.24	10.73	18.93	3.91	102.22
$T_{5,i}$ (s)	99.26	91.27	72.31	75.08	28.09	83.60

water discharge of 43.3 m^3 . The design water level of the upstream reservoir is 70.0 m. The system is composed of one main pipeline, six branch pipelines and five water intakes, and a valve is installed at the end of the branch. The elevation of the main pipeline centerline and positions of the water intakes are shown in Figure 2(b). According to the mathematical model, steady flow of the system is calculated by method of characteristic (MOC). The piezometric head of water intakes are 68.76 m, 68.54 m, 51.93 m, 49.86 m and 40.26 m separately.

Water hammer pressure under different closing laws of multi-valves

Single valve closure

In this section, the effects of single valve closure on the maximum water hammer rise in the 5# water intake are studied. Each valve is closed within 100 s. The transition processes of the system are calculated and analyzed through MOC. Table 2 shows parameters of the time to reach the maximum pressure at the 5# water intake.

From Table 2, both the maximum pressure rise at the 5# water intake and the time of maximum water hammer pressure are different. On the one hand, the reason is that the greater the distance of the valve from the water intake,

the longer it takes for the wave caused by the valve closing to propagate to the water intake.

On the other hand, the greater the distance of the valve from the water intake, the greater the attenuation of the wave during the propagation process. The distance from the 1# valve to the 5# water intake is the farthest, at 71.903 km, and the maximum water hammer pressure rise at the 5# water intake generated by the 1# valve is the smallest. And the distance from the 5# and 6# valve to the 5# water intake is the closest, at 1.193 km and 4.451 km, respectively, and the pipeline discharge of the 6# valve is much larger than the discharge of the 5# pipeline ($8.3 \text{ m}^3/\text{s} \gg 0.8 \text{ m}^3/\text{s}$). Therefore, the maximum pressure rise generated by the 6# valve at the 5# water intake is the largest, at 102.22 m. In addition, according to Table 1, the water velocity of M8 is highest because the diameter is the smallest and the discharge is higher. Therefore, from Table 2, the maximum pressure rise generated by the 4# valve of the M8 at the 5# water intake is the second largest.

Simultaneous valve closure

This is the same as the single valve closure law. Valves of branches are simultaneously closed within 100 s. Figure 3 presents the variations of water hammer pressure at the 5# water intake generated by the simultaneous valve closure.

Figure 3 shows that the superposed maximum pressure at the 5# water intake is 280.42 m. Compared with the piezometric head of 5# water intake, the superposed maximum pressure rise at 5# water intake under the simultaneous

valve closure is 240.16 m ($\Delta H_{5,\text{all}} = 240.16 \text{ m}$). From Table 2, the superposed maximum pressure rise at the 5# water intake under the single valves closure is 145.41 m ($\sum_i^6 H_{5,i} = 145.41$). By comparing the superposed maximum pressure rise at the 5# water intake, it can be believed that the superposed maximum rise under simultaneous valve closure is much larger than that under single valve closure. The reason is that the superposition of water hammer waves is completely ignored under the single valve closure. The result is consistent with the results of previous studies. It shows that the mathematical model and calculation method established in this paper are reasonable.

Effect of sequential valve closure on superposed water hammer pressure of main pipeline

The mathematical model and calculation method established in this paper are verified in the section above. Therefore, these mathematical models can be used to calculate the sequential valve closure. From Table 2, when the valves are closed separately, the time to reach the maximum pressure at 5# water intake has the following relationship. $T_{5,5} < T_{5,3} < T_{5,4} < T_{5,6} < T_{5,2} < T_{5,1}$. Based on Equation (13), the sequential closing times of valves can be written as: $\Delta T_{5,i} = T_{5,1} - T_{5,i}$, $\Delta T_{5,1} = 0$, $\Delta T_{5,2} = T_{5,1} - T_{5,2} = 7.99$, $\Delta T_{5,3} = T_{5,1} - T_{5,3} = 26.95$, $\Delta T_{5,4} = T_{5,1} - T_{5,4} = 24.18$, $\Delta T_{5,5} = T_{5,1} - T_{5,5} = 71.17$, $\Delta T_{5,6} = T_{5,1} - T_{5,6} = 15.66$. When valves are sequentially closed within 100 s, the relationship between the opening of each valve and the time is shown in Figure 4(a). Figure 4(b) presents

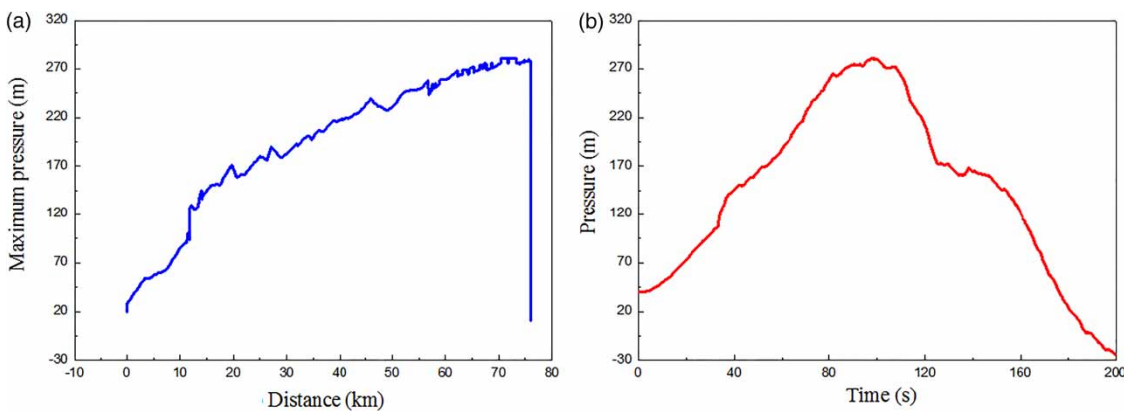


Figure 3 | (a) Maximum pressure curve along the main pipeline under simultaneous closing all of valves, (b) variations of the water hammer pressure at the 5# water intake under simultaneous closing all of valves.

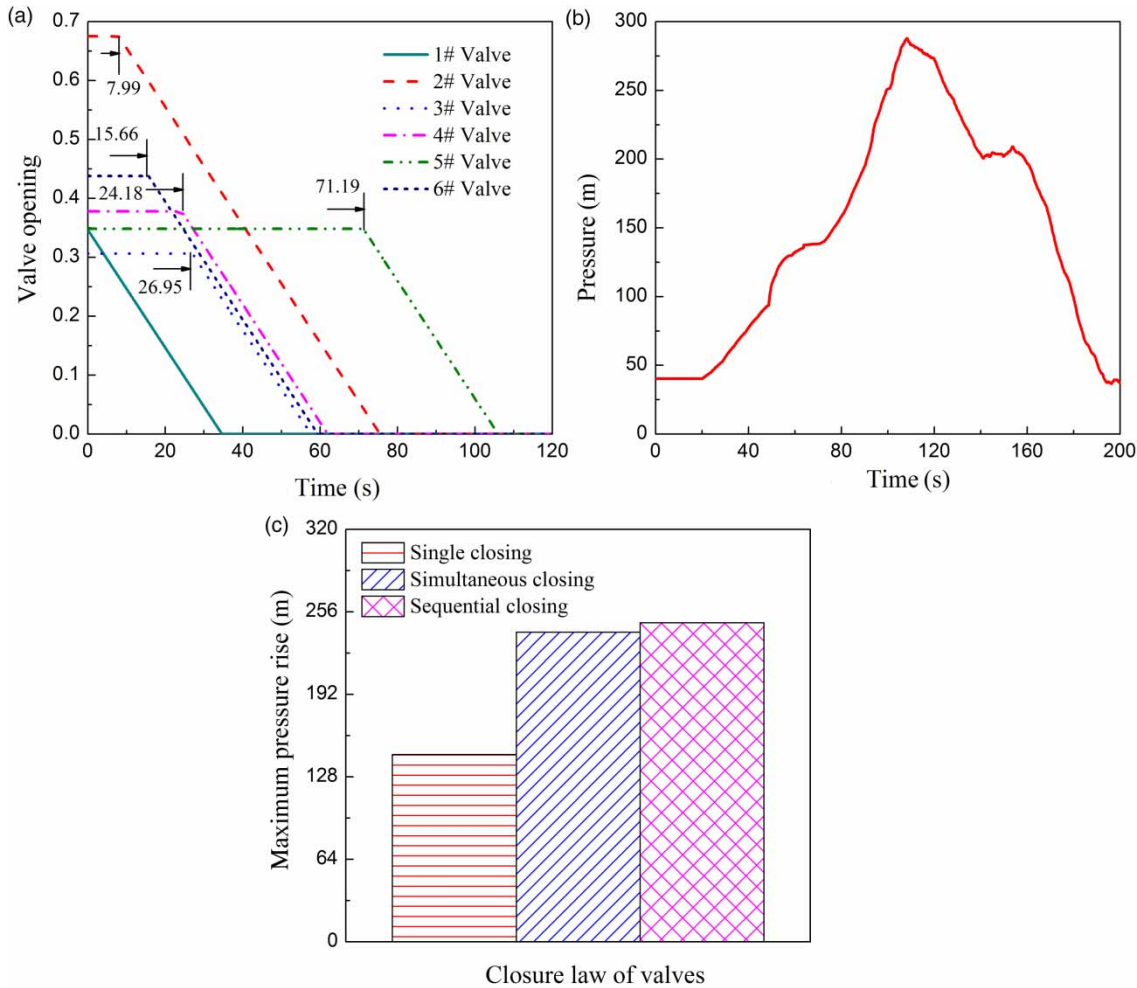


Figure 4 | (a) Laws of sequential valves closure, (b) variations of the water hammer pressure at the 5# water intake under sequential closing, (c) comparison of different valve closure laws.

the variations of the superposed pressure at the 5# water intake under the sequential valve closure.

It can be seen from Figure 4(b), when the valves are closed according to Equation (13), the superposed maximum pressure at the 5# water intake is 287.81 m. Compared with the piezometric head of 5# water intake, the superposed maximum pressure rise is 247.55 m ($\Delta H_5 = 247.55$).

The comparison of the superposed maximum pressure rise at the 5# water intake under the single, simultaneous and sequential valve closure is shown in Figure 4(c). According to the comparison, the superposed maximum pressure rise under the sequential closing is the largest followed by the superposed maximum pressure rise under the simultaneous closing. Then, the superposed maximum pressure

rise under the single valve closure is the smallest. Based on the above analyses, it can be believed that the superposed maximum pressure rise in the main pipeline under sequential closing of Equation (13) is the largest.

Effect of sequential valve closure on superposed water hammer pressure of branch pipelines

In the section above, the effects of sequential valve closure on water hammer pressure of the main pipeline are investigated. The results show that the superposed maximum pressure rise at the main pipeline under sequential valve closure is the largest. According to the propagation of waves, the water hammer wave generated by the valve closing propagates on the main pipeline, as well as on branch pipelines. Therefore,

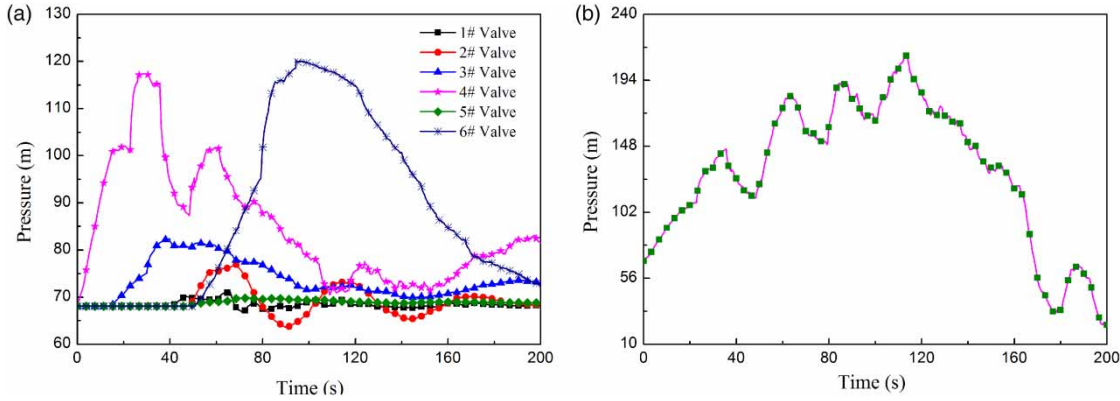


Figure 5 | Variations of water hammer pressure at the end valve of branch M8 under (a) single and (b) simultaneous valves closure (M8 is a branch pipeline as shown in Figure 3(a)).

the laws of the closing valves have an important effect on superposed pressure of the branch pipelines.

In this section, the transition processes of the branch pipeline of M8 are calculated and analyzed. The piezometric head at the end valve of branch M8 is 68.07 m. When the valves are closed within 100 s, the variations of pressure at the end valve of branch M8 under single and simultaneous valve closure are shown in Figure 5. Table 3 presents parameters of the time to reach the maximum pressure under the single valves closure.

From Figure 5(a), compared with the piezometric head of the end valve of branch M8, the superposed maximum water hammer pressure rise is 129.76 m ($\sum_i^6 H_{M8,i} = 129.76 \text{ m}$). And the water hammer pressure rise generated by the 6# valve accounts for 40.31% of the total pressure rise. In addition, according to Figure 5(b), when all valves are simultaneously closed, the superposed maximum water hammer pressure rise is 143.06 m ($\Delta H_{M8,\text{all}} = 143.06 \text{ m}$).

From Table 3, when valves are closed separately, the time to reach the maximum pressure at the end valve of branch M8 has the following relationship. $T_{M8,4} < T_{M8,3} < T_{M8,1} < T_{M8,2} < T_{M8,5} < T_{M8,6}$. Based on Equation (13), the

Table 3 | Parameters of the maximum water hammer pressure rise and time at end valve of branch M8

Valves	1#	2#	3#	4#	5#	6#
The maximum pressure (m)	71.15	76.92	82.42	117.44	69.87	120.38
$H_{M8,i}$ (m)	3.08	8.85	14.35	49.37	1.80	52.31
$T_{M8,i}$ (s)	65.84	68.41	39.85	28.90	69.56	94.31

sequential closing times of valves can be written as $\Delta T_{M8,6} = 0$, $\Delta T_{M8,1} = T_{M8,6} - T_{M8,1} = 28.47$, $\Delta T_{M8,2} = T_{M8,6} - T_{M8,2} = 25.90$, $\Delta T_{M8,3} = T_{M8,6} - T_{M8,3} = 54.46$, $\Delta T_{M8,4} = T_{M8,6} - T_{M8,4} = 65.41$, and $\Delta T_{M8,5} = T_{M8,6} - T_{M8,5} = 24.75$. When valves are sequentially closed within 100 s, the relationship between the opening of each valve and the time is shown in Figure 6(a). Figure 6(b) presents variations of the superposed water hammer pressure at the end valve of branch M8 under the sequential valves closure.

It can be seen from Figure 6(b), when the valves are closed according to Equation (13), the superposed maximum pressure at the end valve of branch M8 is 287.81 m. Compared with the piezometric head, the superposed maximum pressure rise is 281.36 m ($\Delta H_{M8} = 281.36 \text{ m}$).

The comparison of the superposed maximum pressure rise at the end valve of branch M8 by the single, simultaneous and the sequential valve closure is shown in Figure 6(c). According to the comparison, the superposed maximum pressure rise under the sequential closing is the largest, followed by the superposed maximum pressure under the simultaneous closing. Then, the superposed maximum pressure rise under the single valve closure is the smallest. Based on the above analyses, it can be believed that the superposed maximum pressure rise at branch pipeline under sequential closing according to Equation (13) is the largest.

DISCUSSION

In order to investigate the effect of valve closing law on the superposed water hammer pressure of a tree-type long

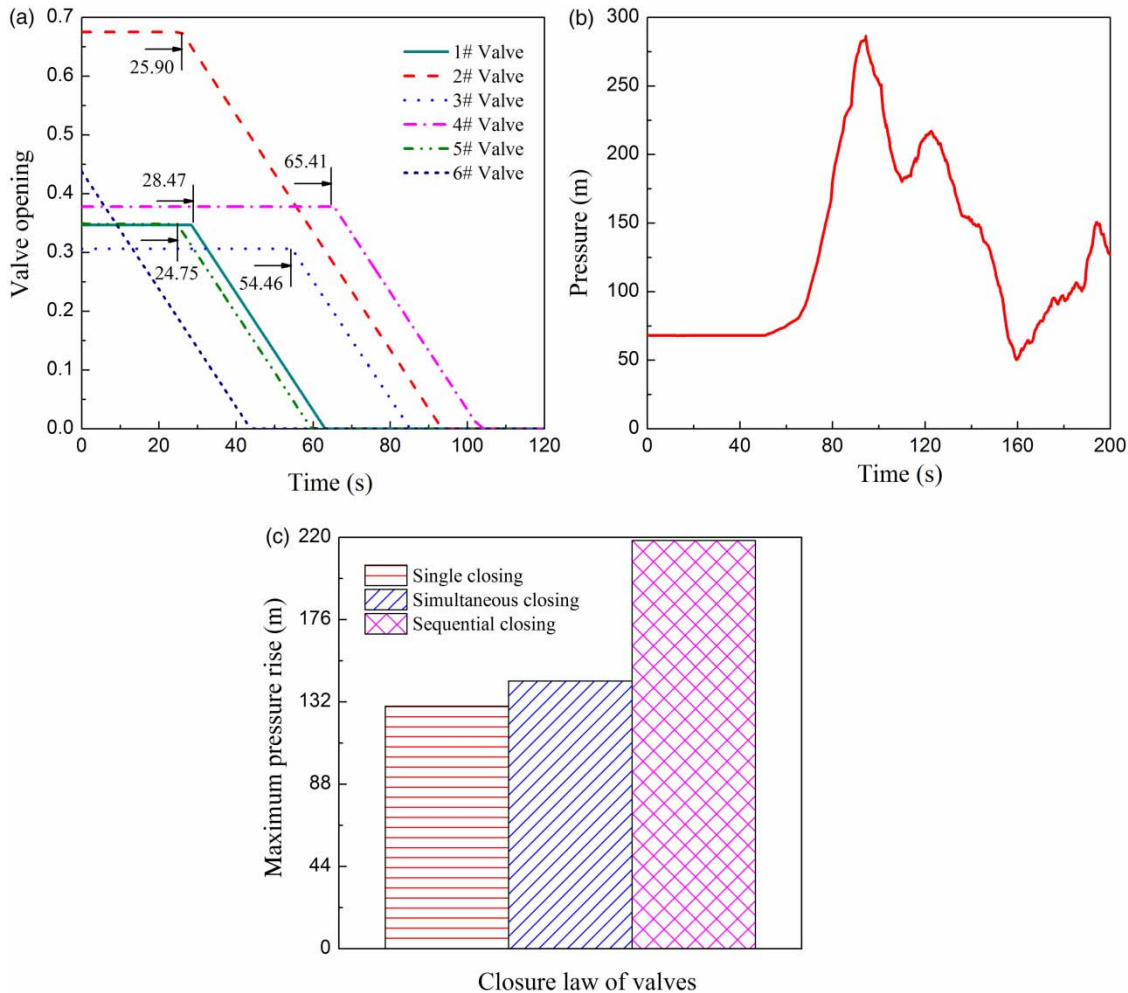


Figure 6 | (a) Laws of sequential valves closure, (b) variations of the superposed water hammer pressure at the end valve of branch M8 under sequential closing, (c) comparison of different valve closure laws.

distance gravitational water supply system, the formula of sequential valves closure is derived. The formula is verified using numerical simulation based on a practical project. In this section, the effect of sequential valves closure on superposed water hammer pressure of the main pipe and branch pipe is discussed.

1. The superposed maximum water hammer pressure rise at the main pipe and branch pipe under the single and simultaneous valves closure are compared separately. The variations of superposed pressure of the main pipe and branch pipe are shown in Figures 4 and 5, respectively. From Figure 4, when valves are closed within 100 s, the superposed maximum pressure rise at

5# water intake of the main pipe under single and simultaneous valves closure is 145.41 m and 240.16 m, respectively. It can be believed that the superposed maximum pressure rise at the main pipe under simultaneous closing is larger than that under single valve closure. Figure 5 also shows that, compared with single valve closure, the superposed maximum pressure rise at the branch pipe under simultaneous closing is the largest. The reason is that the superposition of water hammer waves is completely ignored under the single valve closure. These results are consistent with the results of previous studies.

2. The superposed maximum water hammer pressure rise at the main pipe and branch pipe under the single,

simultaneous and the sequential valve closure are compared separately. The comparison of the results is shown in Figures 4 and 6. Figure 4 indicates that, when the formula of sequential closing ($\Delta T_{j,i} = T_{j,n} - T_{j,i}$) is adopted, the superposed maximum pressure rise at 5# water intake is the largest compared with the single and simultaneous valve closure. Figure 6 also indicates that, when valves are closed within 100 s, the superposed maximum pressure rise at the end valves of branch M8 under single, simultaneous and sequential valve closure is 129.76 m, 143.06 m, and 281.36 m respectively.

The reason is that, in previous works, the propagation and superposition of the waves are ignored. The previous works indicate that the superposition maximum pressure rise produced by simultaneous valve closure is the largest compared with the single valve closure. However, every branch has different distances from the water intakes in tree-type long distance gravitational flow, the time when the waves caused by simultaneous valve closure propagate to the same section is different. Then, because the waves cannot be strengthened, the superposition maximum pressure rise is not the largest. Therefore, when the formula of sequential valves closure is used, which is established based on the propagation and superposition of the waves, the superposed maximum water hammer pressure rise at the main pipe and branch pipe is the largest.

3. The effect of the sequential valve closure on the superposed maximum pressure rise at the main pipeline and the branch pipeline are compared. The superposed maximum pressure rise generated by sequential valve closure at the main pipeline and the end valve of branch M8 are shown in Figures 4(b) and 6(b), respectively. The superposed maximum pressure rise at the main pipeline under the sequential closing is 2.98% larger than the simultaneous closing. The superposed pressure rise at the end valve of branch M8 under the sequential closing is 34.48% larger than the simultaneous closing. Compared with the superposed maximum pressure rise at the main pipeline, it can be believed that the effect of sequential valve closure on the superposed maximum pressure rise at the branch pipeline is more sensitive.

CONCLUSIONS

For a tree-type long distance gravitational water supply system, in this paper, the sequential valve closure formula was proposed based on the propagation and superposition of waves. The formula was verified using numerical simulation. The results showed that the formula agrees well with the numerical results. In addition, the superposed maximum water hammer pressure rise at the main pipe and branch pipe were compared under the single, simultaneous and sequential valve closure. Based on the results, the main conclusions were drawn as follows. First, compared with the superposed maximum pressure rise under the single and simultaneous valve closure, the maximum pressure rises at main pipeline and the branch pipeline under the sequential valve closure were the largest. Second, compared with the superposed maximum pressure rise at the main pipeline, it can be believed that the effect of sequential valves closure on the superposed maximum pressure rise at the branch pipeline is more sensitive.

This paper proposes that the sequential valve closure is the most unfavorable condition of the tree-type long distance gravitational water supply system, which is more dangerous than conventionally simultaneous valve closure. In actual operation, it is necessary to avoid this valve regulation. Besides, it must be pointed out that the water hammer waves caused by valves are only investigated from the propagation and superposition of the wave in this paper, and other factors are not considered. Therefore, future research is needed on the impact of other factors on the superposed water hammer pressure.

ACKNOWLEDGEMENTS

This study was supported by the National Natural Science Foundation of China (Grant Nos 51879087 and 51839008), the Postgraduate Research & Practice Innovation Program of Jiangsu Province (Grant No. 2019B71114 and SJKY19_0492), and the fifth '333 Project' of Jiangsu Province (Grant No. BRA2018061).

REFERENCES

- Bostan, M., Akhtari, A. A. & Bonakdari, H. 2018 Deriving the governing equation for a shock damper to model the unsteady flow caused by sudden valve closure and sudden demand change. *Journal of Water Supply: Research and Technology—Aqua* **67** (2), 202–210.
- Chaudhry, M. H. 2014 *Applied Hydraulic Transients*. Springer, New York.
- Fan, J. L., Wang, J. D., Zhang, X., Kong, L. S. & Song, Q. Y. 2019 Exploring the changes and driving forces of water footprints in China from 2002 to 2012: a perspective of final demand. *Science of the Total Environment* **650**, 1101–1111.
- Lai, Z. N., Qian, L., Karney, B., Yang, S., Wu, D. Z. & Zhang, F. X. 2018 Numerical simulation of a check valve closure induced by pump shutdown. *Journal of Hydraulic Engineering* **144** (12), 06018013-1-9.
- Liao, Y. Y., Lian, Z. S., Feng, J. L., Yuan, H. B. & Zhao, R. H. 2017 Effects of multiple factors on water hammer induced by a large flow directional valve. *Strojniski Vestnik—Journal of Mechanical Engineering* **64** (5), 329–338.
- Miao, D., Zhang, J., Chen, S. & Yu, X. D. 2017 Water hammer suppression for long distance water supply systems by combining the air vessel and valve. *Journal of Water Supply Research and Technology—Aqua* **66** (5), 319–326.
- Moghaddas, S. M. J. M., Samani, H. M. V. & Haghighi, A. 2017 Multi-objective optimization of transient protection for pipelines with regard to cost and serviceability. *Journal of Water Supply: Research and Technology—Aqua* **66** (5), 340–352.
- Wan, W. Y. & Li, F. Q. 2016 Sensitivity analysis of operational time differences for a pump-valve system on a water hammer response. *Journal of Pressure Vessel Technology* **138** (1), 011303.
- Wang, Y., Zhang, J. & He, C. 2017 Valve close plan optimization of long-distance gravity flow water-supply project. *Yellow River* **39** (5), 142–146.
- Wang, X. T., Zhang, J., Yu, X. D. & Shi, L. 2018 Research on the water hammer protection of the air vessel caused by underground pipe burst in long distance water supply system. *MATEC Web of Conferences* **246**, 1066.
- Wylie, E. B., Streeter, V. L. & Suo, L. 1993 *Fluid Transients in Systems*. University of Michigan, Englewood Cliffs.
- Xiao, J., Wang, L. Q., Deng, L. & Jin, Z. D. 2019 Characteristics, sources, water quality and health risk assessment of trace elements in river water and well water in the Chinese Loess Plateau. *Science of the Total Environment* **650**, 2004–2012.
- Xu, H., Guang, Z. M. & Qi, Y. Y. 2011 Hydrodynamic characterization and optimization of Contra-push check valve by numerical simulation. *Annals of Nuclear Energy* **38** (6), 1427–1437.
- Zhang, Z. 2019 Wave tracking method of hydraulic transients in pipe systems with pump shut-off under simultaneous closing of spherical valves. *Renewable Energy* **132**, 157–166.
- Zhang, B. R., Wan, W. Y. & Shi, M. S. 2018 Experimental and numerical simulation of water hammer in gravitational pipe flow with continuous air entrainment. *Water* **10** (7), 928.

First received 25 February 2019; accepted in revised form 1 May 2019. Available online 10 June 2019